COMPUTER SIMULATION OF THE DISLOCATION ENSEMBLE KINETICS IN THE ELASTIC FIELDS OF MESODEFECTS AND FRAGMENTATION PROCESSES DURING PLASTIC DEFORMATION

V.N. Perevezentsev[1,2*], G.F. Sarafanov[1,2], J.V. Svirina[1]

[1]Mechanical Engineering Research Institute, Russian Academy of Science,

Belinskogo 85, Nizhni Novgorod, 603024, Russia

[2]Lobachevsky State University of Nizhni Novgorod, Gagarina 23, Nizhni Novgorod, 603950, Russia

*e-mail: pevn@uic.nnov.ru

Abstract. The analysis of the elementary processes of fragmentation (broken sub-boundaries and a misorientation band formation) is performed by the discrete dislocation computer simulation method. It is shown that a fragmentation driving force is a decrease of the system energy due to the dislocations redistribution in the elastic field of primary mesodefects (disclinations, dipoles of disclinations et al.) accumulating on the grain boundaries and triple junctions during plastic deformation. The comparison of the results with the results obtained by continual approach is made. The misoriented structures formation inside shear bands during plastic deformation of mono-crystals is considered. It is shown that this process is similar to the polycrystal fragmentation, but in this case dislocation clusters accumulating near shear band interface act as the primary mesodefects. An analysis of conditions of low-angle sub-boundaries trasformation into medium-angle boundaries is performed.

1. Introduction

It is known that the strain-induced refinement (fragmentation) of the material structure i.e., a division of initial grains grains of polycrystals into finer mutually misoriented regions surrounded by low-, medium- and high-angle boundaries is usually observed during plastic deformation [1].

Experimental and theoretical studies of the fragmentation [1, 2] show that its origin in polycrystals is due to the nonuniform plastic deformation as in the body of the grain or in the ensemble of grains of the polycrystal. It is found, that plastic incompatibilities induced by plastic deformation (such as disclinations, dipoles of disclinations and pile-ups of misorientional misfit dislocations) accumulate on the grain boundaries and triple junctions and create the system of primary mesodefects [3-5].

An increase of the primary mesodefects power induces collective effects in the ensemble of moving lattice dislocations. The mesodefects long-range stress fields disturb lattice dislocation flow, make it non-homogeneous and, in the end, generates broken sub-boundaries (secondary mesodefects) in the adjacent grain regions. Namely, the broken dislocation boundaries (individual or in the form of misorintation bands) are typical experimentally observed rotational defects. Usually the broken sub-boundaries can be considered as partial disclinations in many cases according to [2-6]. The increase of the primary mesodefects power leads to the broken sub-boundaries propagation and the formation of a subgrain structure during plastic deformation.

Basic elements of fragmented structure are investigated in the framework of the continual kinetic approach [7-12]. It is shown that primary mesodefects generate areas with increased dislocation density and dislocation charge. Such redistribution of dislocations effectively screen elastic fields of mesodefects, reduces system energy and creates conditions for appearance of broken sub-boundaries.

Despite the rigor of the obtained solutions, the continual consideration can not describe the regularities of the dislocation ensemble evolution during the broken boundaries formation and the stability of the formed structures after the external load off.

Thereby in this paper the results of the investigation of the dislocation ensemble behavior and the formation of secondary mesodefects are summarized in the framework of an alternative approach based on a discrete dislocation computer simulation method.

The main purposes of the present work are the analysis of the elementary processes of fragmentation by the discrete dislocation computer simulation method, the comparison of the results with the results obtained by continual approach and demonstration of a possibility to apply computer simulation method to the analysis of the misoriented structures appearing inside shear bands during plastic deformation of FCC crystals.

2. A model of the dislocation ensemble dynamics

A method of 2D and 3D discrete dislocation dynamics simulation was widely used to describe the deformation behavior of mono- and poly-crystals [13-19]. Below we will use 2D discrete dislocation dynamics concept developed by van der Giessen and Needleman [20] to investigate the dislocation ensemble dynamics under the influence of the mesodefects elastic fields.

Each dislocation is characterized by the Burgers vector $b^{(s)}$, parallel to the direction of dislocation slip, the coordinates ($x^{(s)}$, $y^{(s)}$) and velocity ($v_x^{(s)}$, $v_y^{(s)}$), s = 1, . . ., N, where N is the number of dislocations. The contribution of inertial summands to the equation of dislocation motion is negligible in comparison with the dynamic friction. Taking it into account the equation of the dislocation motion for the dislocation s in the quasi-viscous approximation may be written as

$$v_k^{(s)} = \frac{dx_k^{(s)}}{dt} = M_{ki} e_{ijm} l_j b_n^{(s)} (\sigma_{mn}^{ext} + \sigma_{mn}^{int}), \qquad (1)$$

where σ_{mn}^{ext} is the tensor of the external stress; σ_{mn}^{int} is the tensor of the internal stress defined as the sum of all Peach–Koehler interactions with all other defects; M_{ki} is the tensor of mobility with nonzero diagonal elements that specify slip and climb dislocation mobility; e_{ijm} is the unit anti-symmetric tensor; l_j is the unit vector tangent to the line of dislocation.

Below we consider the case, when the deformation is controlled by the dislocation slip. On a further investigation step in some cases a dislocation climb is taken into account. In the model it is assumed that plastic deformation in the grain initiates at some critical shear stress σ_c in one of the selected slip system. Since the elastic stress field $\hat{\sigma} = \{\sigma_{xx}, \sigma_{yy}, \sigma_{xy}\}$ is essentially non-homogeneous the deformation initiates locally and then spreads in neighboring regions of the grain.

This pecularity of plastic deformation is provided by threshold dislocations generation. The dislocations multiplication in the volume of the grain is characterized by some rate $\dot{N}$ of generation of unlike dislocations pairs in the slip planes. Dislocations in the pair are placed on the distance $x_c = Db/\sigma_c$ (here σ_c is the threshold stress of a Frank–Read source, $D = G/[2\pi(1-\nu)]$, G is a shear modulus, ν is a Poisson ratio [21]). Their annihilation takes

place at the stresses below the threshold stress σ_c.

The coordinates of the dislocation pair are randomly generated in accordance with a uniform distribution law. In absence of the defects of disclination type it leads to a homogeneous dislocations distribution in the body of the grain.

A recombination processes are taken into account in the model. Annihilation of the unlike dislocations moving towards each other is characterized by their capture cross-section $S_a = \pi x_a^2/4$, where $x_a = 0,25\,x_c$.

3. Screening of the disclination elastic field by an ensemble of moving discrete dislocations

In the present section the results of computer simulation of the plastic deformation are performed under the same conditions as it is used in the continual kinetic approach [7].

A disclination with a power $\omega = 0.02$ were placed in a center of a rectangular region with a size $(d \times d)$, where $d = 2\,\mu m$. The evolution of the lattice dislocation ensemble in the field of the external stress $\sigma_{xy}^e = 0.002\,D$ and the elastic field of disclination is investigated during $2000\,s$.

The mobility of dislocations in their slip plane along $0x$ axis is chosen to provide typical strain rate values. Thus, for the dislocations density $\rho \approx 5\cdot 10^9\,cm^{-2}$ and the strain rate $\dot{\varepsilon} = b^2 \rho M \sigma_{xy}^e \approx 10^{-3}\,s^{-1}$ the value of mobility is $M \sim 10^5\,D^{-1}s^{-1}$.

The results of the simulation are shown in Fig. 1. The distribution of the dislocations in the grain comes to a statistically stationary state at the moment of time $t \approx 500\,s$ and the dislocation structure takes a form shown in Fig. 1.
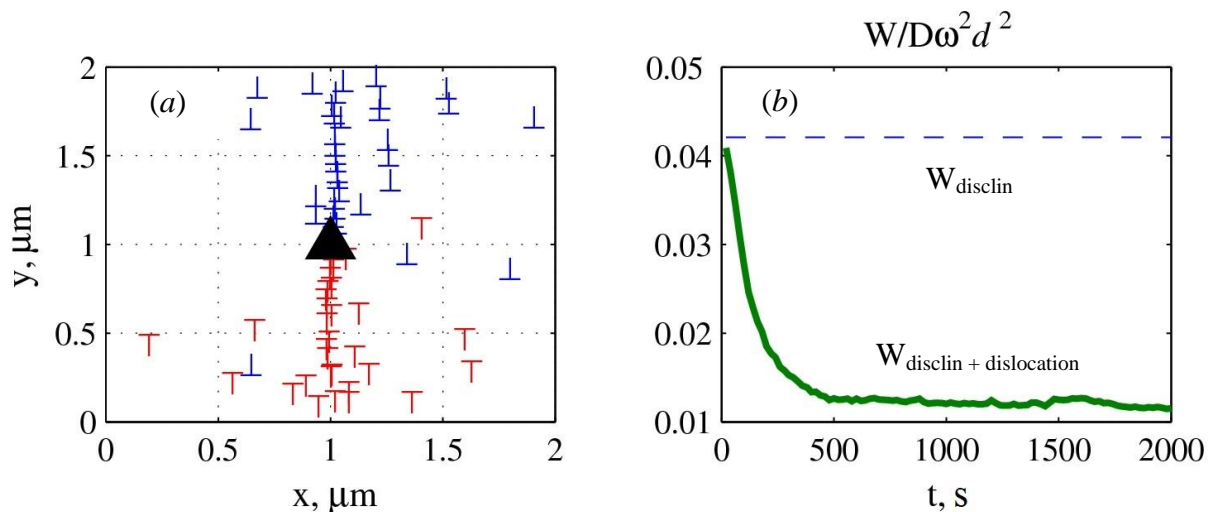

Fig. 1. Screening of the elastic field of disclination with the power $\omega = 0.02$ by sub-boundaries formed during plastic deformation: (a) − a stationary dislocation structure in a form of unlike sub-boundaries at the moment of time $t = 2000$ s; (b) − the evolution of a total energy changes W in the region $(d \times d)$ (the energy of disclination $W_{disclin}$ is plotted by the dotted line). W and $W_{disclin}$ are normalized to the value $D\omega^2 d^2$.

To a specified point of time $t \approx 500\,s$ the calculated values take the stationary quantities, characterized by their mean values. The mean dislocation density in the grain is $\rho = 4\cdot 10^9\,cm^{-2}$, total energy of the system is $W_e = 0.012\,D\omega^2 d^2$ (Fig. 1b).

It is important to note that the elastic energy of disclination W_{disclin} essentially exceeds the energy of the screened system W (Fig. 1b). Dislocations redistribute in the elastic field of disclination to provide a decrease of total energy of the system.

This result has a good correlation with the result obtained in the continual consideration [7]. A spatial distribution of the elastic energy density is performed in Fig. 2 for the continual kinetic approach [7] and for computer simulation for the same region (2×2) μm. As it is seen from Fig. 2, the screening effect in the framework of continual kinetic approach gives the value $W / W_{\text{disclin}} \approx 0.3$ and the computer simulation gives a close value $W / W_{\text{disclin}} \approx 0.33$ (Fig. 2).

Thus, the computer simulation the same as the continual approach confirm that the elastic field of disclination can be effectively screened by en ensemble of moving dislocations.
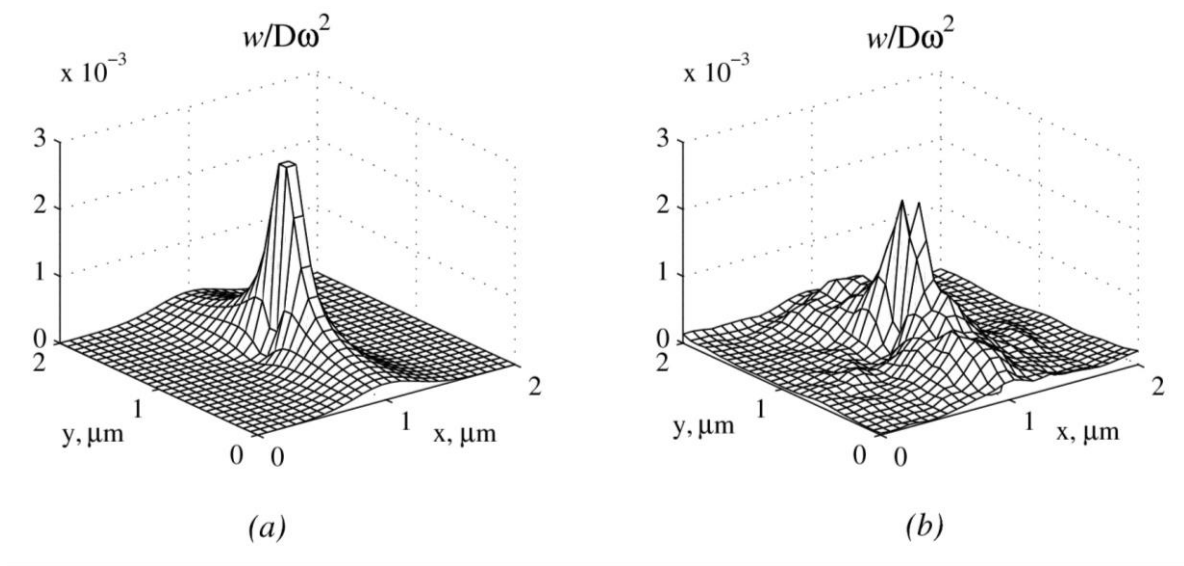

Fig. 2. The elastic enegry density of the system normalized to the value $D\omega^2$: (a) the continual approach [7]; (b) computer simulation.

4. Simulation of the dislocation ensemble kinetics and sub-boundaries formation in the elastic field of disclination placed on the grain boundary

The investigation of the dislocation ensemble dynamics in the elastic field of disclination is performed in a rectangular region with a size $(d \times d)$, where $d = 2\,\mu$m. However, in contrast to the pervious section (s. 3), disclination was placed on the boundary of grain (see Fig. 3a). One slip system oriented along $0x$ axes is considered. The mobility of dislocations is taken as in the previous section.

Let us consider the evolution of an ensemble of dislocations in the field of a wedge disclination with a power $\omega = 0.02$ and the external field $\sigma_e = \sigma_c = 0.003D$. Other parameters have the following values: $x_c = Db / \sigma_c = 0.1\,\mu$m, $\dot{N} = \dot{N}_+ = \dot{N}_- = 0.1$ is a dislocation generation rate, $N(0) = 2$ (initial number of dislocations).

At $t_p = 300$s the external field was switched off to investigate the stability of the broken sub-boundary formed during previous plastic deformation.

The evolution of dislocation structure at various moments of time is shown in Fig. 3. The corresponding changes of the structure parameters are performed in Fig. 4. Deformation in the grain starts in its left part (see Fig. 3b, Fig. 4d). After a period of time $t_y \approx 50$ s the

system comes to the stationary state. The dislocations density and the sub-boundary misorientation reach their mean values $\rho \approx 5 \cdot 10^9$ cm^{-2} and $\theta_{st} \approx 0.01$ correspondingly (see Fig. 3c). Then deformation in the right part of the grain starts (see Fig. 4d). The strain rate in the right part of the grain is leveling with the strain rate in the left part ($\dot{\varepsilon}_{right} = \dot{\varepsilon}_{left} \approx 0.7 \cdot 10^{-4}$s^{-1}).
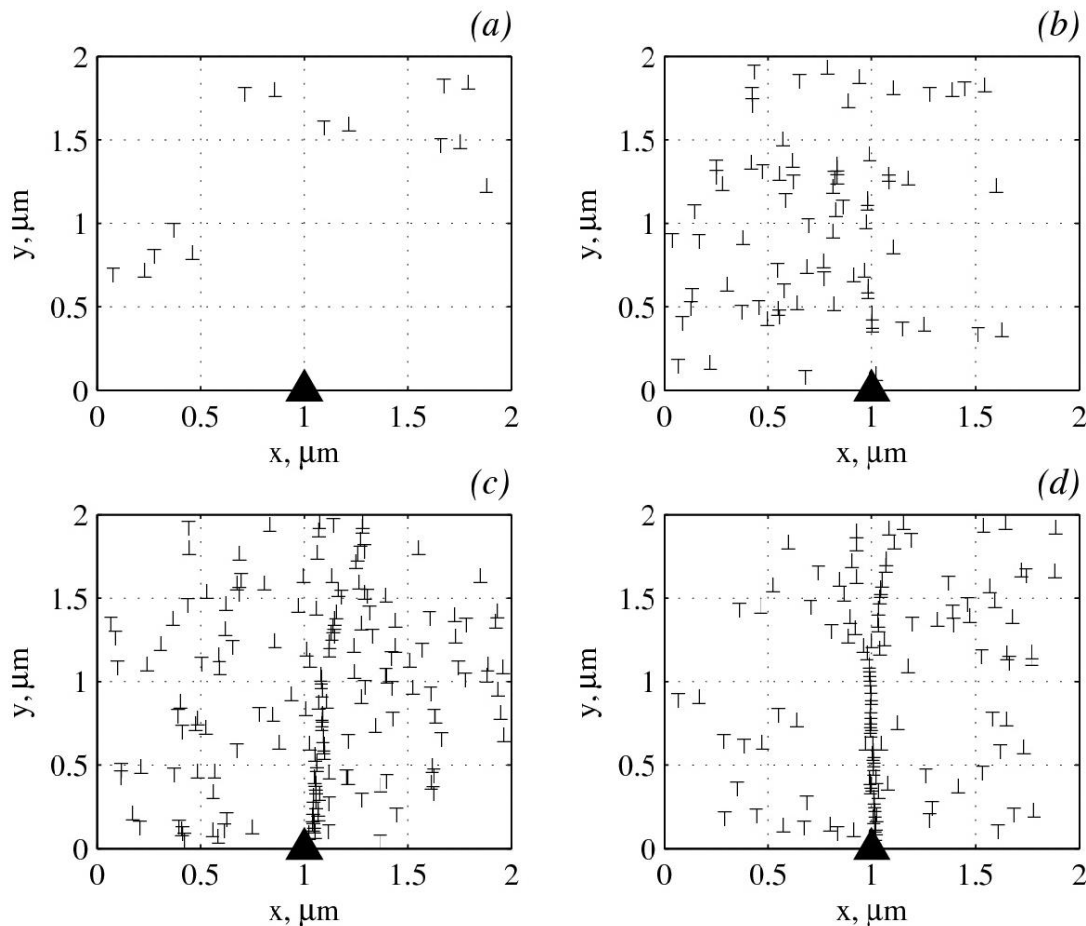

Fig. 3. The evolution of a dislocation ensemble in the field of a disclination with power $\omega = 0,02$ and in the external stress field σ_e at various moments of time:
$(a) - t = 1$ s, $\sigma_e = 0.003D$; $(b) - t = 10$ s, $\sigma_e = 0.003D$; $(c) - t = 250$ s, $\sigma_e = 0.003D$;
$(d) - t = 500$ s, $\sigma_e = 0$.

The dislocations distribution has the dynamic nature, but in the stationary state ($t_y < t < t_p$) it does not change statistically. A typical distribution for this case (at $t = 250$ s) is shown in Fig. 3c. Corresponding statistical characteristics are performed in Fig. 4. The histogram of the unlike dislocations number (N_+ и N_-) with respect to x is shown in Fig. 4a, the histogram of the sub-boundary misorientation value θ_{st} with respect to y is shown in Fig. 4b (sub-boundary width was taken as $\Delta x_{st} = d/5$).

It is seen that disclination forms a region of spatially localized dislocation charge which can be considered as a dynamic sub-boundary with a misorientation $\theta_{st} \approx \omega/2$.

The sub-boundary stationarity means that on the average the sub-boundary loses and absorbs the same number of dislocations per a unit of time. At the same time the sub-

boundary has the evident features of quasi-stable configuration.

The most clearly it can be seen when the external field is switched off (at $t > t_p$). As it follows from Fig. 4c, the sub-boundary misorientation does not change while the dislocations density decreases. Deformation stops (Fig. 4d) some dislocations sink on the grain boundaries, the sub-boundary takes the equilibrium configuration (Fig. 3d) with the minimum of the system potential energy.
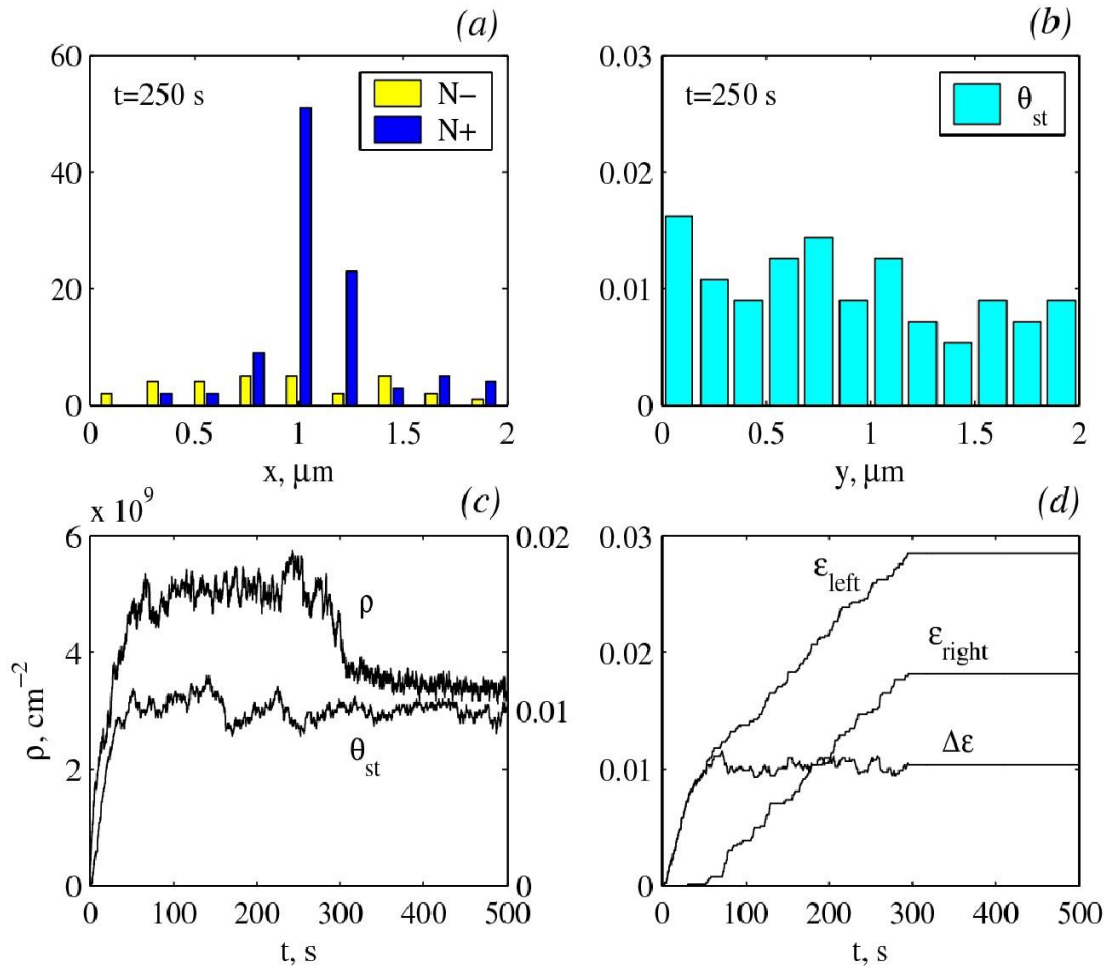

Fig. 4. Distribution of dislocations, sub-boundary characteristics, and instantaneous strain values ($\sigma_e = 0$ at $t > 300\,\text{s}$): (a) – the histogram of the unlike dislocations number distribution (N_+ and N_-) with respect to x at $t = 250$ s; (b) – histogram of the sub-boundary misorientation value θ_{st} with respect to y at $t = 250$ s; (c) – time evolution of the dislocations density and the sub-boundary misorientation θ_{st}; (d) – time evolution of the strain value of the left (ε_{left}), right (ε_{right}) parts of the grain and the strain difference ($\Delta\varepsilon = \varepsilon_{left} - \varepsilon_{right}$).

The distinctive feature of the sub-boundaries is their formation in a form of broken sub-boundaries (Fig. 3c, d) often ending by a "faculae" of dislocations (Fig. 3d).

5. Simulation of a misorientation band formation

It is shown in the experimental research [1, 2] that a misorientation band (a dipole structure consisting of a two parallel dislocation boundaries) extending into the grain body from a double ledge of high angle grain boundary is typical structural element that is observed in

plastic deformed materials. From theoretical point of view the misorientation band forms due to the primary disclination dipole dissociation with an emission of dipole of partial disclinations into the grain. In the framework of the static disclination approach it is found that misorientation band formation is energetically favorable [22]. However the kinetics of the process of misorientation band formation is not considered.

Let us note, that under static conditions the unlike dislocations enter into the broken sub-boundaries located not parallel to each other. This is illustrated by the results of simulation of the dislocations rearrangement from their initial quasi-homogeneous distribution (at a dislocations density $\rho = 2.5 \cdot 10^9 \mathrm{cm}^{-2}$) under the influence of the elastic field of a primary disclination dipole (Fig. 5a). The matter is the zero level lines of dipole stress field σ_{xy}, along which dislocation boundaries tend to arrange, diverge at a right angle in the absence of the external field (Fig. 5b).
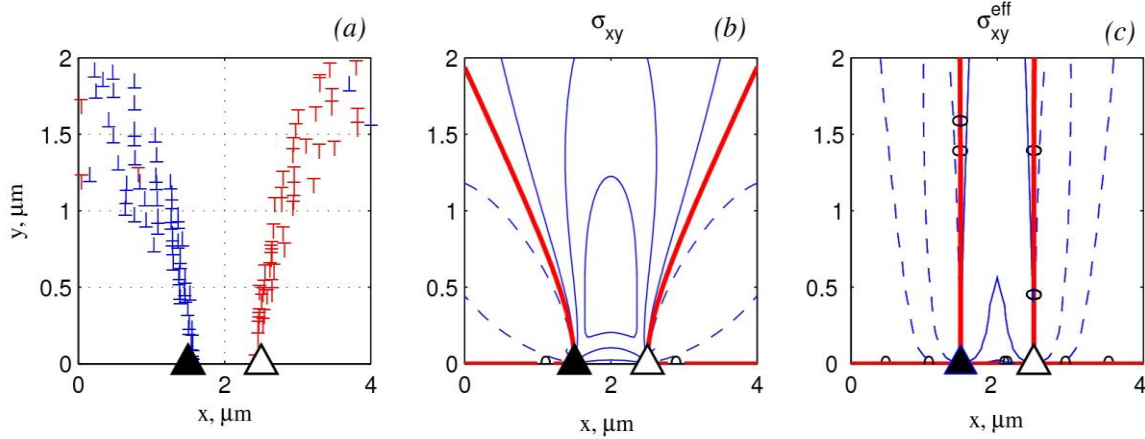

Fig 5. (a) – the equilibrium dislocation structure formed from the initial homogeneous distribution in the elastic field of disclination dipole with power $\omega = 0.02$; (b) – zero level lines of stress field tensor shear component σ_{xy} of non-screened disclination dipole; (c) – zero level lines of stress field tensor shear component σ_{xy} of screened disclination dipole.

Similar results were obtained for the formation of an equilibrium dislocation structure in a weak external field ($\sigma_e \leq D\omega/2$). Thus, it is impossible to explain the misorientation band formation in the framework of a static approach.

Therefore the misorientation band formation have to be considered in the framework of the kinetic approach. Earlier it was demonstrated in the framework of continual approach [7]. It was shown that the zero level lines of the stress tensor component σ_{xy}^{eff} screened by the ensemble of moving dislocation are almost parallel to each other (Fig. 5c).

The computer simulation of dislocation ensemble evolution in the field of disclination dipole (with a power ω and shoulder $2a = 1\,\mu\mathrm{m}$) is performed in [23] with the account of its kinetics. The investigation was performed inside a two-dimensional rectangular area $(d \times 2d)$, where $d = 2\,\mu\mathrm{m}$ under conditions $\sigma_c = 3 \cdot 10^{-3} D$, $\sigma_e = \sigma_c/3$. It was assumed, that initially the disclinations power linearly increases with the rate $\dot\omega = (2/3) \cdot 10^{-4}\mathrm{s}^{-1}$ from zero up to $\omega_{max} = 0.02$ during the period of time $t_p = 300\,\mathrm{s}$. Later ω remains constant ($\omega = \omega_{max}$) during $t = 300$ s.

At the initial period of time ($0 < t < t_1 \approx 60\,\mathrm{s}$) there is no deformation in the grain. All generated dislocations annihilate. At $t > t_1$ a multiplication of lattice dislocations starts under

the influence of increasing elastic field of disclinations (Fig. 6c). The disclination field captures lattice dislocations and forms the sub-boundaries (Figs. 6a, b).
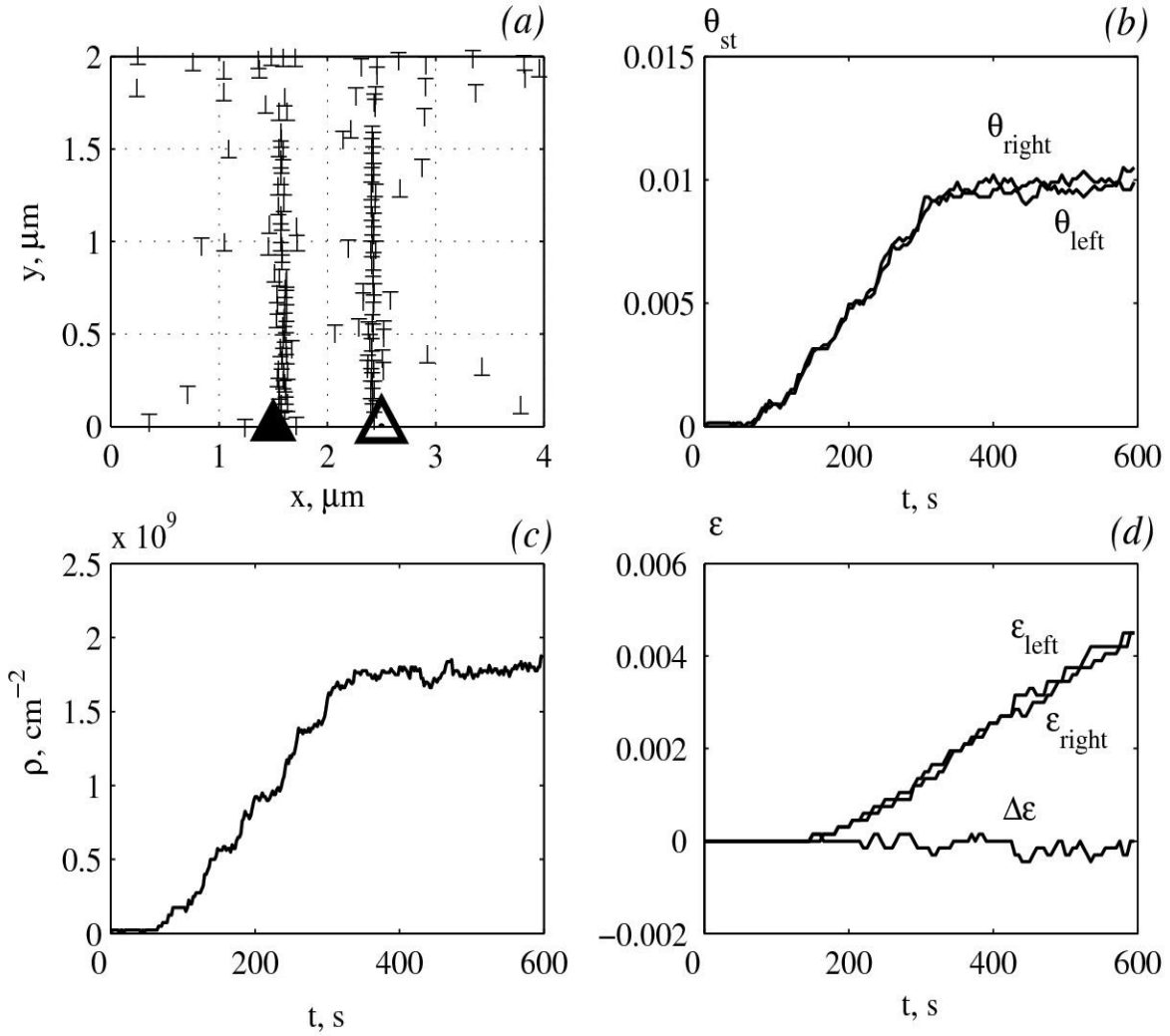

Fig. 6. The results of simulation with the account of dislocations kinetics:
(a) − a dislocation structure formed as a dipole system of broken sub-boundaries (incomplete misorientation band) in the external field $\sigma_{xy}^e = 0.001D$ and in the elastic field of the disclination dipole with power $\omega = 0.02$;
(b) − time evolution of the sub-boundaries misorientation;
(c) − time evolution of the dislocation density in the body of the grain;
(d) − time evolution of the strain value.

At time $t = t_2 \approx 200$ s deformation becomes relatively homogeneous. Dislocations reach side surfaces and on the contrary to the results of the previous section $\varepsilon_{right} \approx \varepsilon_{left}$ (Fig. 6d). In the period of time $t_1 < t < t_p \approx 500$ s a mean dislocations density in the grain increases proportionaly to the disclination power increase (Fig. 6c). Also the sub-boundaries misorientation increases linearly:

$$\theta_{st}(t) \approx \frac{1}{2}(\omega(t) - \omega(t_y)). \tag{2}$$

At $t > t_p = 300\,\text{s}$ the disclination power stops to increase and in the aftermath the sub-boundary misorientation and the dislocations density growth also stops (Fig. 6b, c). As a result a system of unlike parallel sub-boundaries with misorientation $\theta_{st} \approx \omega/2$ forms (Fig. 6a). Let us note, that when the sub-boundaries misorientation stops to increase, the strain value increases with the same rate (Fig. 6d). It means that the strain value is controlled by the external stress field σ_e.

Thus, it is shown that the system of unlike parallel sub-boundaries with a misorientation $\theta_{st} \approx \omega/2$ forms in the elastic field of disclination dipole under the kinetics conditions (i.e. with the account of dislocations generation, annihilation and sink). Sub-boundaries are disposed normally to the acting slip plane at a distance equal to the disclination dipole shoulder. The obtained results confirm the assumption that both misorientation bands and isolated broken sub-boundaries form under conditions of the developed dislocations kinetics.

Above the formation of a misorientation band was considered in the case when dipole of disclinations were plased in the plain grain boundary in artificial way. In the framework of the kinetic approach we investigate now the conditions of the misorientation band formation near a disclination dipole that induced on a grain boundary double ledge by plastic deformation. Let us consider the case, when disclination dipole is induced by an interaction of a shear band with the grain boundary in a model bicrystal (Fig. 7a).
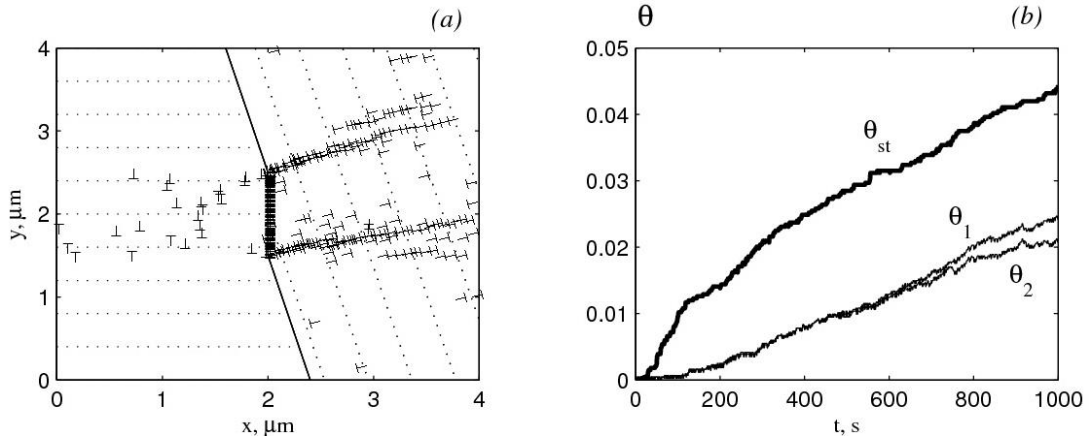

Fig. 7. (*a*) A dislocation structure formed at a time $t = 1000\,\text{s}$; (*b*) time evolution of primary disclination dipole misorientation θ_{st} on the grain boundary ledge and sub-boundaries misorientations θ_1 and θ_2.

It was assumed that dislocations in each grain move along the one slip system (along $0x$ in the left grain and at an angle of 105° to $0x$ in the right grain). Axis of tension is chosen to provide the absence of external stress shear component on the slip system in the right grain. Thus, dislocations there move under the influence of the internal stresses.

The lattice dislocations incoming on the grain boundary from the left grain form there a dipole of disclinations. After a while (at $t \approx 100\,\text{s}$) the formation of a mesodefect causes an accommodative plastic deformation and a formation of the broken sub-boundaries in the right grain.

It is seen that the power of disclinations $\omega = \theta_{st}$, accumulating on the intergranular boundary comes to the value $\omega \approx 0.04$, while the sub-boundaries misorientations are $\theta_{1,2} \approx 0.02$. Similar to the previous section, the universal relation $\theta = \omega/2$ between the power of initial mesodefect ω and sub-boundaries misorientation θ is valid. This conclusion correlates with the results obtained in the framework of kinetic continual approach.

6. The formation of a dipole sub-boundaries system in the elastic field of a planar mesodefect

A primary planar mesodefect is a system of equidistantly distributed on the grain boundary orientation misfit dislocations with a tangential component of the Burgers vector. This type of mesodefects accumulates on the intergranular boundaries during plastic deformation [7]. In the framework of the continual approach it was shown, that planar mesodefect may induce a misorientation band formation similar to the disclination dipole [7].

Below we consider the results of computer simulation of the dislocation ensemble evolution and the misorientation band formation in the elastic field of this type of mesodefects. An investigation was performed for two cases. In the first case the dislocations kinetics, i.e. dislocation generation and annihilation were not considered. Only sink on side surfaces was taken into account. At the initial time dislocations in the grain were distributed quasi-homogeneously with a density $\rho_0 = 2.5 \cdot 10^9 \, \text{cm}^{-2}$. Then a weak external stress field $\sigma_{xy}^e = 0.001D$ and a mesodefect stress field $\sigma_{xy}^{(m)}$ were switched on. Some dislocations sink on side surfaces under the influence of total stress field $\sigma_{xy} = \sigma_{xy}^e + \sigma_{xy}^{(m)}$, the dislocations density value decreases. The remaining dislocations inside the grain take the equilibrium configuration.

The equilibrium dislocation structure is represented by the sub-boundaries forming along the zero level lines of total stress field. In this case the sub-boundaries are located at a certain angle to each other. Thus, a misorientation band does not appear (Fig. 8a).

Let us consider another case, when the kinetic processes (generation, annihilation etc.) are taken into account. Time evolution of the dislocation ensemble was investigated at the following parameters values: $\Omega = 0.01$, $L = 1 \mu m$, where Ω is a mesodefect power (i.e. a linear density of tangential components of the Burgers vector), L is a mesodefect length,

$$\sigma_c = 3 \cdot 10^{-3} D, \qquad \sigma_e = \frac{1}{3} \sigma_c, \qquad x_c = Db / \sigma_c = 0.1 \, \mu m, \qquad x_a = 0.09 \, \mu m, \qquad y_a = 0.01 \, \mu m,$$

$\dot{N} = \dot{N}_+ = \dot{N}_- = 0{,}1 \, \text{s}^{-1}$, $N(0) = 2$ (initial number of dislocations). The elastic field of mesodefect was switched on at $t_1 = 75 \, \text{s}$. A time of simulation is 600 s.

Time evolution of the dislocation structure and its characteristics are shown in Fig. 8. At the initial period of time ($0 < t < t_1$), when only the weak external field $\sigma_{xy}^e = \sigma_e$ acts, plastic deformation does not take place. All lattice dislocations generated inside the grain annihilate. At a time $t = t_1$ dislocations multiplication (Fig. 8c) and opposite sign dislocation sub-boundaries formation start (Fig. 8a, b).

The lattice dislocation system had a form of clusters in a non-stationary state (till the time $t_s \approx 200 \, \text{s}$). In the stationary state it has a form of the misorientation band, i.e. parallel unlike dislocation sub-boundaries (Fig. 8b). The sub-boundaries misorientation value is equal to $\theta \approx 0.012$ (Fig. 8d), a distance between the sub-boundaries is $2a \approx 0.4 \, \mu m$ (Fig. 8b).

On the basis of the continual approach [12] the misorientation of such sub-boundaries was evaluated as $\theta = \Omega L / (4a)$. Taking into account the obtained by simulation value $a \approx 0.2 \, \mu m$, and initial parameters $\Omega = 0.02$ and $L = 1 \, \mu m$ one can find

$$\theta = \frac{\Omega L}{4a} = 0.0125 . \tag{3}$$

It is very close to the value of sub-boundary misorientation $\theta = 0.012$ received by simulation (Fig. 8d).
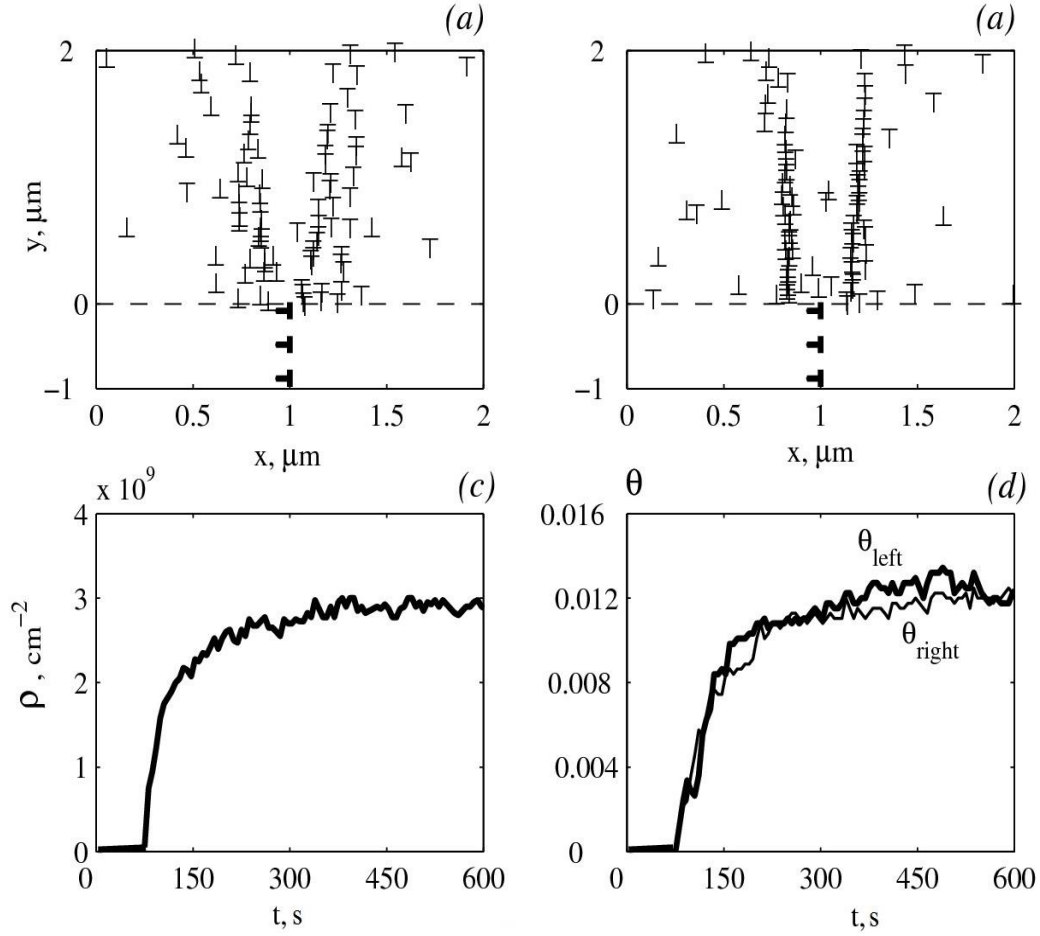
Fig. 8. Time evolution of the dislocation structure and its characteristics under the influence of the external field $\sigma^e_{xy} = 0,001D$ and the field of planar mesodefect with a power $\Omega = 0.02$: (*a*) — a dislocation structure at $t = 100$ s ; (*b*) — a dislocation structure in a form of misorientation band at $t = 600$ s ; (*c*) — time evolution of dislocation density value ρ ; (*d*) — time evolution of the sub-boundaries misorientation θ .

7. Fragmentation in a tri-crystal

An investigation of the self-consistent mesodefects and sub-boundaries formation in a model tri-crystal and a grain fragmentation is performed in the present section. The mesodefects and sub-boundaries formation were investigated inside a rectangular area $(d \times d)$, where $d = 4\,\mu$m in the case of uniaxial loading with $\sigma_e = \sigma^{(e)}_{yy} = 10^{-3}G$. Simulation time was $t = t_e = 800$ s. At a time $t = t_e/2$ the external loading is switched off.

The following parameters were chosen for the simulation: slip planes in a left grain are oriented by an angle 30^0 with respect to $0x$ axis, in a right grain they are parallel to the $0x$ axis, in an internal grain slip planes are oriented by an angle -10° with respect to $0x$ axis. For the considered case plastic deformation initiates in the left grain under the influence of the external stress $\sigma_e = \sigma^{(e)}_{yy}$. A shear stress in the slip planes τ_e of the right grain is zero. In the internal grain its value is too low $\tau_e < \sigma_c$ to satisfy the dislocations generation condition.

The dislocation structure formed at a time $t = t_e$ is presented in Fig. 9. It is represented by two unlike sub-boundaries fragmenting the initial internal grain into three mutually misoriented subgrains.

As it is mentioned above, fragmentation is initiates by the primary mesodefects induced by plastic deformation. The mesodefect accumulating on the intergranular boundaries are the disclinations and the planar mesodefects, which cause accommodative plastic deformation by their elastic fields and finally equalize strain rates in the adjacent grains.

The mesodefects types and powers of disclinations $\omega_1, \omega_2 ... \omega_8$ and planar mesodefects $\Omega_1, \Omega_2 ... \Omega_8$ were found for the structure shown on the Fig. 9.

Fig. 9. A dislocation structure in the tri-crystal formed in the elastic field of mesodefects induced on the initial intergranular boundaries by plastic deformation.

It is interesting to consider the influence of mesodefect type on the structure formation. First, let us consider a dislocation structure that forms only in the field of junction disclinations. The results of simulation are performed in Fig. 10a.
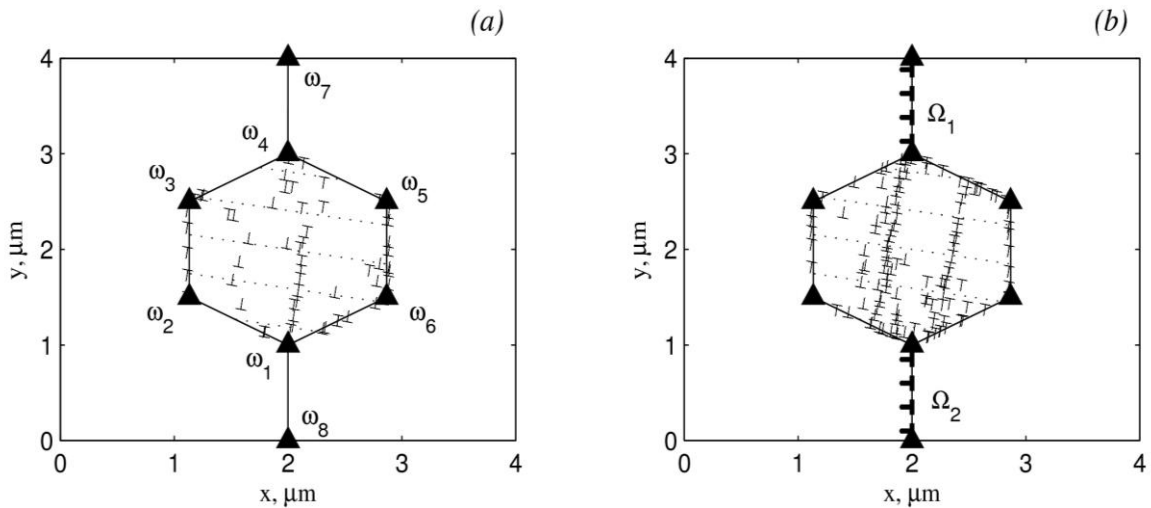

Fig. 10. A dislocation structure formed in the fields of the induced mesodefects: (*a*) — junction disclinations with powers $\omega_1 = -0.01$, $\omega_2 = 0.006$, $\omega_3 = 0.004$, $\omega_4 = -0.0041$, $\omega_5 = -0.0046$, $\omega_6 = 0.0015$, $\omega_7 = 0.005$, $\omega_8 = 0.0075$; (*b*) — junction disclinations supplemented by two planar mesodefects with powers $\Omega_1 = -0.0024$ and $\Omega_2 = 0.011$.

As it is seen from Fig. 10a, only single broken sub-boundary forms in the field of disclinations that is not sufficient for the description of the structure, shown in Fig. 9.

Simulation shows that a supplementation of junction disclination system by other (planar) mesodefects with the powers Ω_1 and Ω_2 (see Fig. 10b) leads to the formation of the dislocation structure similar to the structure shown in Fig. 9. Thus, the presence of the planar mesodefects is also important for the grain fragmentation.

8. Computer simulation of a shear band fragmentation in cupper single crystal

Single crystals have no grain boundaries containing primary mesodefects. So, for the considered case a subdivision of the material into areas with different orientations is due to the interaction of lattice defects at different length scales and non-homogeneous dislocation structures formation. Therefore, it is necessary to investigate a self-consistent motion of the dislocation ensemble to describe a microstructure formation. Let us consider this process on an example of shear bands fragmentation in cupper single crystal.

Shear bands are typical structures that observed in the deformed materials. Experimental researches show that the internal band structure usually has transformations during plastic deformation. Thus, the band subdivides into areas with different orientations [24].

EBSD map of a band microstructure (Fig. 11) shows that a band structure appears in a deformed copper single crystal [24]. Shear bands have an internal substructure in a form of stripes with local misorientations (Fig.11) that are located almost perpendicularly to the primary slip plane. The slip systems inside (primary system A) and outside the shear band (secondary system C) were determined in [24].
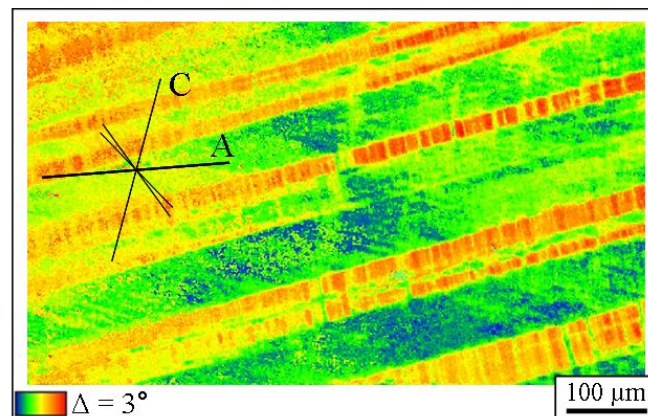

Fig. 11. EBSD map of a band microstructure in a deformed copper single crystal
(shear strain ~ 23 %) [24].

Let us assume that plastic deformation initiates inside the shear bands on the slip system A (primary slip system). Since the dislocation dipoles formation inside the shear band leads to the hardening, the external stress increase activates the secondary slip system C. As it is shown in [25], local reactions between the dislocations of the slip systems A and C lead to the formation of sessile dislocations (Lomer–Cottrell locks) (see Fig. 12).

In the considered case there are no physically determined boundaries between the shear band and the surrounding material, therefore locks formation can take place in the whole volume of the band. However, if the density of dislocations in the primary slip system is sufficiently high at a time of secondary slip system activation, the reactions take place in some layer with length L and width Δ near the interface between the band and the surrounding material. As a result the dislocation charge clusters accumulate in this layer and may act as the primary mesodefects.
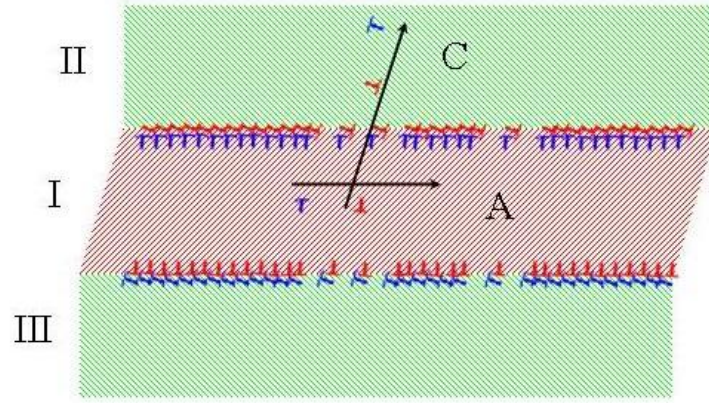
Fig. 12. Schematic illustration of the shear band dislocation structure.

The dislocations clusters in the interface between areas I and II and I and III (Fig. 12) can be considered as a superposition of dislocation systems with a tangential and normal to the band interface Burgers vector components.
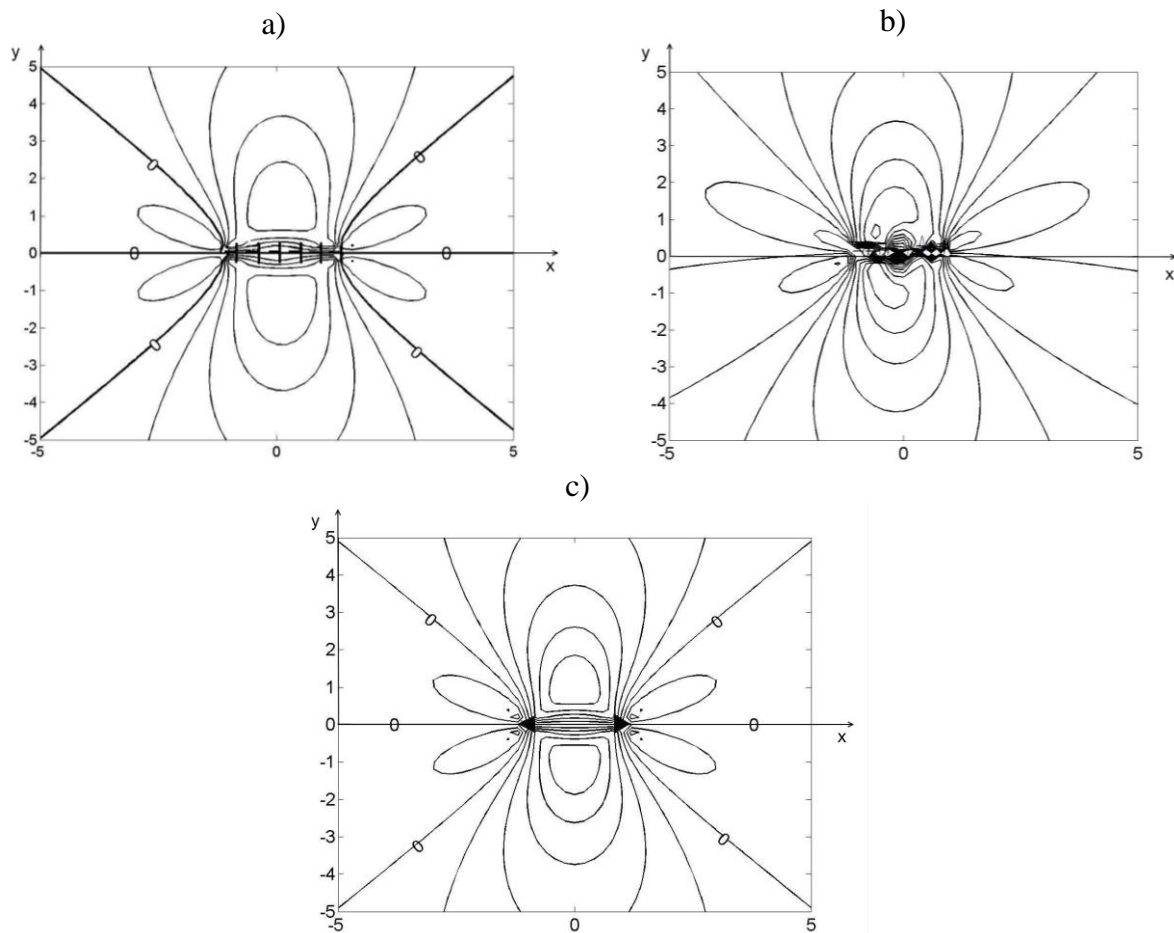

Fig. 13. Profiles of constant fields of shear stresses for (a) the equidistantly arranged discrete dislocations with a Burgers vector density value 0.01; (b) random distribution of the same number of dislocations in a layer $\Delta = 0.2$ μm; and (c) biaxial dipole of wedge disclinations with a power of 0.01 rad.

As it is seen from Fig. 13 the elastic fields of dislocations clusters with normal Burgers vector components in the layer with width $\Delta \ll L$ can be described in a good approximation as

the elastic field of broken sub-boundaries or the disclination dipoles field with a power ω and shoulder L.

It is seen from Fig. 14 that the elastic fields of tangential components of dislocations accumulated on the band interface along the distance L in the layer with width Δ can be described as the planar mesodefect elastic field.
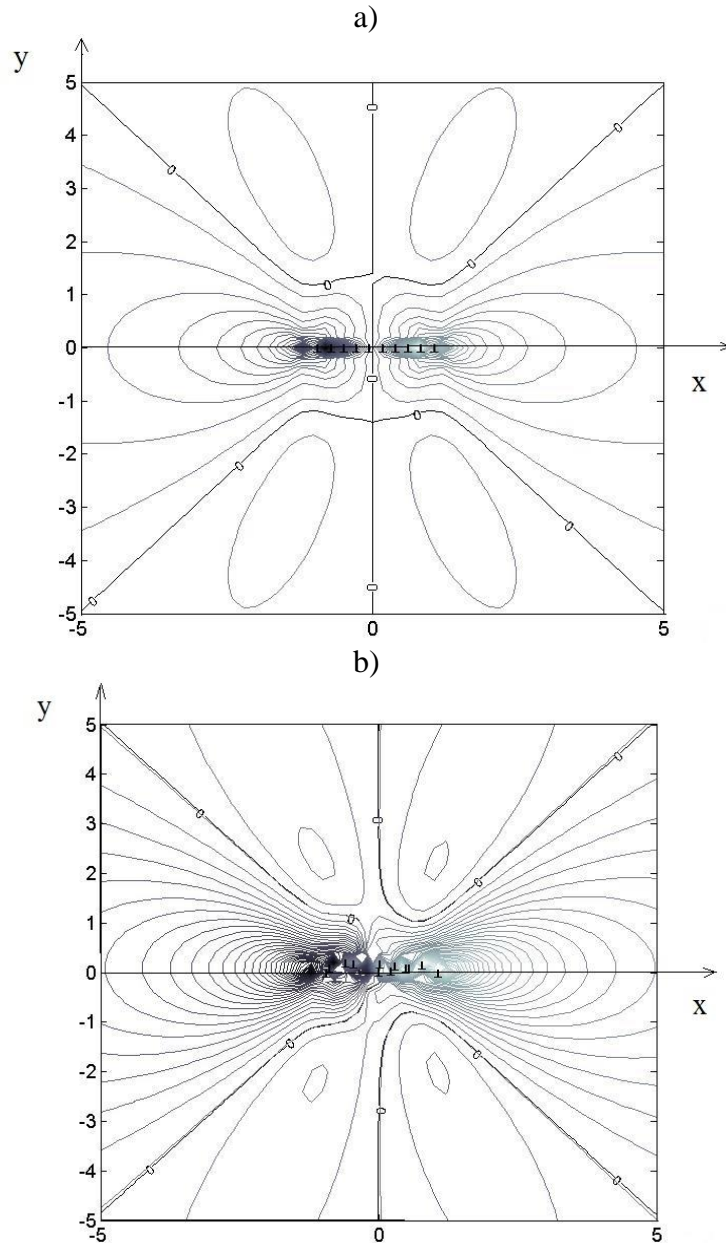
a)

b)

Fig. 14. Profiles of constant fields of shear stresses for (a) a planar mesodefect with a Burgers vector density value 0.01; (b) a planar mesodefect with a random distribution of the same number of dislocations in a layer Δ = 0.2 μm.

The analysis shows that the elastic field of dislocation cluster formed on the band interface can be considered as a superposition of the disclination dipole and the planar mesodefect elastic fields. Taking into account the results received in the previous sections it is possible to assume that the dislocations motion in the fields of this mesodefects will lead to the formation of broken sub-boundaries inside the band, arranged perpendicularly to the primary slip system. Let us illustrate it on the example of sub-boundaries formation inside the

shear band in copper single crystal [24].

Using a locks distribution in the band interface calculated from the experimental data as the initial condition discrete dislocation simulation was performed. The parameters for dislocations annihilation and generation were chosen similar to the previous sections. The external stress value was $\tau = 30$ MPa. The width of the band was 20 μm. The appropriate amount of locks at the interface was calculated from the EBSD map. The areas with high dislocation density 3×10^{13} m^{-2} (the red areas in Fig. 15a) and the low dislocation density 1×10^{13} m^{-2} (the yellow areas, Fig. 15a) are arranged in accordance to the structure of an exemplarily chosen part of the band (Fig. 15a). Inside each area, the locks are distributed randomly. The lengths L of the areas vary from 10 μm to 20 μm. Thus, the clusters of locks within the interface layer ($\Delta \ll L$) can be considered as the system of abovementioned mesodefects.

The results of simulation are performed in Fig. 15b. It is seen that the calculated misorientations have a good correlation with the experimental data (Fig. 15).
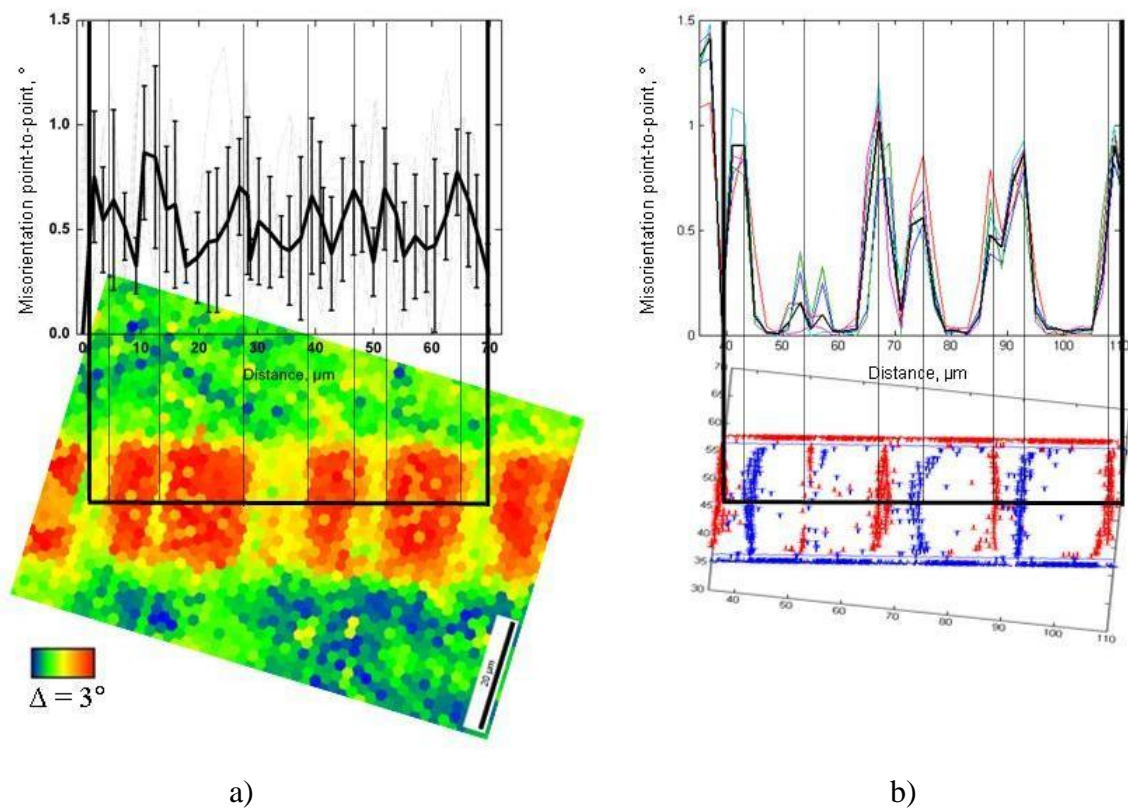

a)   b)

Fig. 15. a) The point-to-point misorientation values within the selected area along the shear band. b) Dislocation arrangement and misorientation values obtained by the dislocation dynamics simulation [26].

9. An analysis of conditions for fragments with medium-angle boundaries formation in shear bands

In the previous sections only the initial stages of fragmentation, i.e. the formation of broken low-angle boundaries in the elastic field of mesodefects was considered.

In the present section an analysis of conditions of low-angle sub-boundaries trasformation into medium-angle boundaries is performed for the particular case when plastic deformation is localized in shear bands. A subdivision of the shear bands into fragments separated by medium-angle and high-angle boundaries was observed experimentally for a number of fcc and bcc metals and alloys [26, 27].

A computer simulation was performed in [28] taking into account dislocation motion along three slip systems. If slip systems are oriented at the angles $\alpha = 0^\circ$, $\beta = 60^\circ$ and $\gamma = -60^\circ$ to the $0x$ axis correspondingly the reactions between α and β dislocations lead to the formation of Lomer-Cottrell locks in the materials with low stacking fault energy [25]. Sink take place on the free surfaces of the crystal. An orientation of loading axis is chosen to provide dislocation motion only in the primary slip system α with the largest value of Schmid factor at the initial moment of time. Plastic deformation initiates in a shear band with a width $h = 0.2\,\mu m$.

Parameters of the model are chosen to provide a constant strain rate condition. Generation and annihilation parameters are taken similar to the previous sections. It is assumed that plastic deformation along all slip system is also localized in the shear bands.

Calculations were performed for a crystal of size $(d \times d)$, where $d = 1\,\mu m$. A shear band thickness was taken similar to the experimental value $0.2\,\mu m$ [26]. The external stress value is $\sigma = 3 \cdot 10^{-3} G$, $\sigma_c = 2,5 \cdot 10^{-3} G$, Burgers vector $b = 3 \cdot 10^{-8}$ cm and dislocation mobility $M = 10^{-4} \text{Pa}^{-1}\text{s}^{-1}$, tensile stress axix was oriented at the angle 30° to the shear band. Time evolution of the dislocation structure is shown in Fig. 16.

At the initial moment of time dislocations move only in the primary shear band (see Fig. 16a). The interaction of unlike dislocations inside the band leads to the formation and accumulation of immobile dislocation dipoles inside the band and, as a consequence, to the hardening that requires an increase in the external stress for further deformation. When the external stress exceeds a threshold value a dislocation motion in the secondary shear bands initiates (see Fig. 16b).

The dislocations of the secondary slip system reach the primary shear band and react with the dislocations of primary slip system that leads to the formation of the sessile dislocations (Lomer–Cottrell locks). As it was shown in the previous section, barrier dislocations accumulate in the vicinity of the band interface on a certain segment of length l. Accumulation of locks at the band interface leads to the increase of the internal elastic fields produced by tangential (to the primary slip system) dislocation components of Burgers vector and to suppression of plastic flow in the secondary shear bands. Relaxation of these fields may occur due to the activation of the accommodation slip system III (see Fig. 16c).

The elastic field of mesodefects, forming on the shear bands interface perturbs the laminar flow of dislocations in the primary band. It leads to the appearance of the dynamic sub-boundaries and the subgrain formation (Fig 16c). A dislocation density in the subgrain boundaries and their misorientation increase with deformation.

A dislocation structure at a time $t=300$ s is shown in Fig. 16d. It corresponds to the strain value $\varepsilon \sim 16$ % in the secondary shear band. Despite the fact that the considered sub-boundaries have the dynamic nature, the formed subgrain is stable after unloading. To confirm this, the dislocation structure after unloading and further relaxation during the time $\Delta t = 50$ s is shown in Fig. 16e. The structure does not essentially change for longer periods of relaxation time Δt. Note, that dislocation walls are still not ideal after relaxation. However an additional annealing leads to the appearence of more regular boundaries (Fig. 16f). In the present work the annealing was simulated as a dislocation structure rearrangement both by dislocation slip and climb under the influence of the internal stresses.

The subgrain boundaries misorientations increase during plastic deformation and reach the value 4.5° at $t=300$ s (Fig. 17). It is important to emphasize, that the misorientation of vertical (ω_1) and horizontal (ω_2) boundaries are not equal. Thus, in the subgrain junctions there is a mismatch of plastic rotations: $\Delta\omega = \omega_2 - \omega_1$. As a result unlike wedge disclinations with power $\Delta\omega$ are accumulated in the junctions and form a disclination quadrupole.
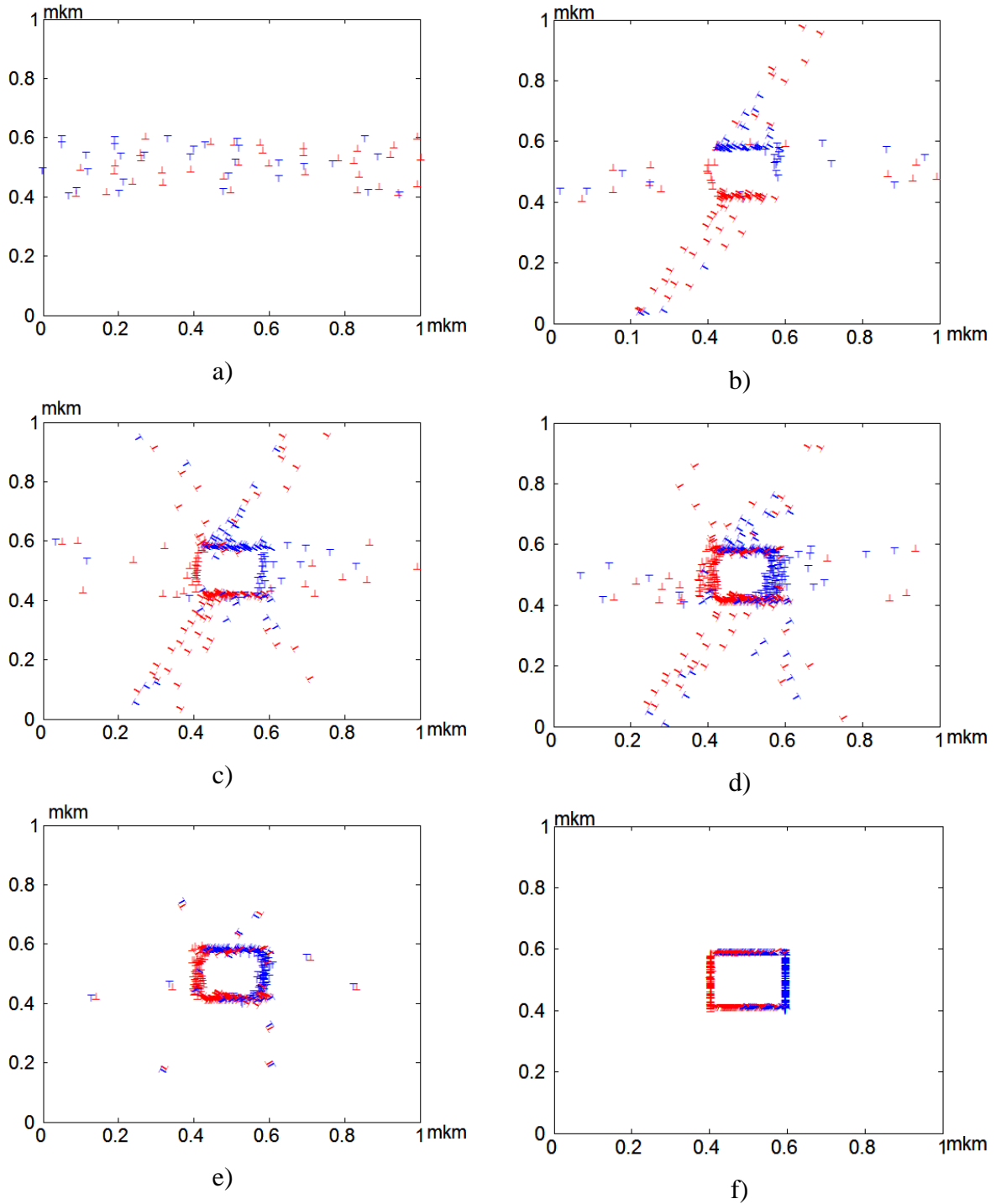
Fig. 16. Dislocation structure formed at the time a) t=50 s, b) t=100 s, c) t=150 s, d) t=300 s, e) without external loading during t=50 s, f) after annealing.

Wherein a mean power of disclination quadrupole $\Delta\omega$ increase with deformation time t and reach a saturation value of the order 0.005 rad (Fig. 17).

Calculations for larger strain values do not qualitatively change the overall picture, i.e. the sub-boundaries misorientations increase at a constant disclinations power value $\Delta\omega$.

Let us consider the reasons of transformation of low-angle boundaries into medium- and high-angle boundaries. A formation of the disclination quadrupole with a power $\Delta\omega = \omega_2 - \omega_1$ leads to the appearance of the internal stress acting opposite to the external stress inside the subgrain.
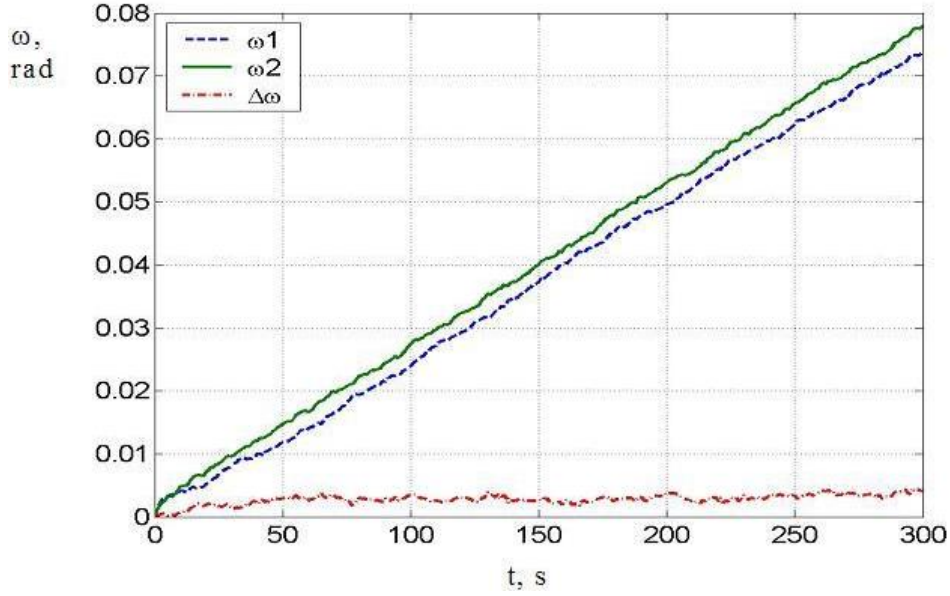
Fig. 17. Misorientation of vertical (ω_1) and horizontal (ω_2) subgrain boundaries and a mismatch of plastic rotations $\Delta\omega$ in the subgrain junctions.

A time-evolution of the total external and internal shear stresses σ_{xy}^{Σ} averaged over the length of the quadrupole (subgrain) is performed in Fig. 18. Elastic field fluctuations are due to the dynamic nature of the dislocation structure. The value σ_{xy}^{Σ} decreases with the increas of disclinations power and at some value $\Delta\omega$ becomes lower than the threshold value $\sigma_c = 2.5 \cdot 10^{-3} G$. Therefore a dislocation generation and their motion directed along the external stress are suppressed inside the subgrain.
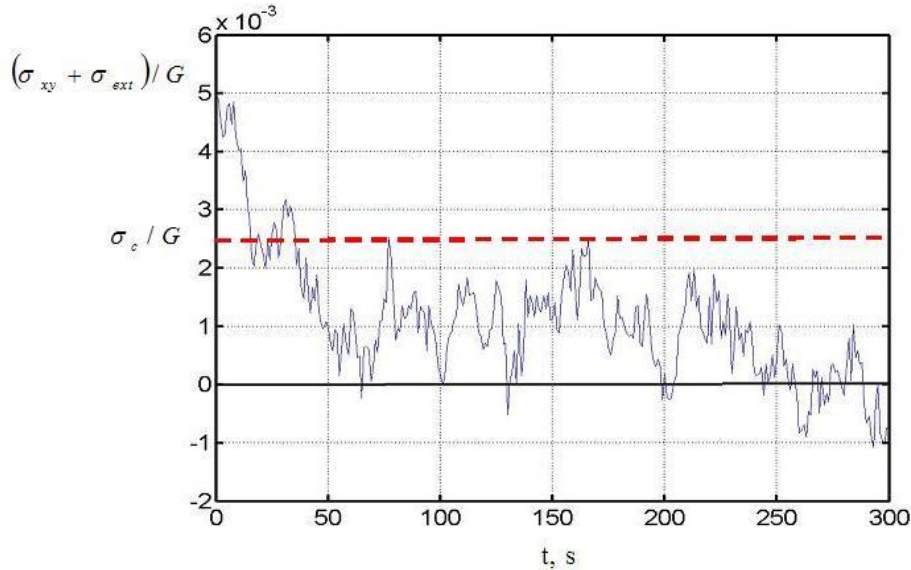

Fig. 18. Time-evolution of the total external and internal shear stresses σ_{xy}^{Σ} averaged over the length of the quadrupole. σ_c is the threshold stress of dislocation source.

Nevertheless the dislocations continue to move outside the subgrain. The dislocation flows incoming into the sub-boundaries increase their misorientations. In other words when a

quadrupole with a constant power $\Delta\omega$ is formed it provides a self-consistent plastic rotation on the subgrain boundaries. So, the subgrain misorientation constantly increase, that leads to the transformation of initially low-angle dislocation boundaries into medium- and high-angle boundaries.

Under the abovementioned conditions the subgrain behaves like an undeformed inclusion in the deformed matrix and has a crystallographic rotation. In terms of dislocation theory it can be described as a formation of the self-consistent dislocation walls along the subgrain perimeter.

10. Summary
Let us note the main results, obtained in the framework of the discrete dislocation computer simulation method.
1. The broken sub-boundaries are formed in the external stress and elastic fields of primary mesodefects. Dislocation sub-boundaries have the dynamic nature and remain stable after unloading.
2. The sub-boundaries formation effectively screens elastic fields of mesodefects. It leads to the system energy and elastic stress gradients decrease that equalize strain rates in the grain volume.
3. The results of computer simulation have a good correlation with the results obtained by continual approach for steady state condition of deformation.
4. The misoriented structures formation inside primary shear band is due to mesodefects (dislocation clusters) accumulating during plastic deformation in its interface at the intersection with secondary shear bands.
5. It is shown that the main condition for the transformation of low-angle dislocation structures into a medium-angle and high-angle boundaries is the suppression of active plastic deformation in a subgrain by the elastic fields of disclinations appearing in subgrain boundary junctions.

References
[1] V.V. Rybin, *Large plastic deformations and fracture of metals* (Metallurgia, Moscow, 1986) (in Russian).
[2] V.V.Rybin // *Problems of Material Science* **33** (2003) 9.
[3] A.N. Orlov, V.N. Perevezentsev, V.V. Rybin, *Grain boundaries in metals* (Metallurgia, Moscow, 1980) (in Russian).
[4] V.N. Perevezentsev, V.V. Rybin, V.N. Chuvil'deev // *Acta Metallurgica et Materialia* **40** (1992) 895.
[5] V.V. Rybin, A.A. Zisman, N.Yu. Zolotorevsky // *Acta Metallurgica et Materialia* **41** (1993) 2211.
[6] A.E. Romanov, A.L. Kolesnikova // *Progress in Material Science* **54** (2009) 740.
[7] V.N. Perevezentsev, G.F. Sarafanov // *Reviews on Advanced Materials Science* **30** (2012) 73.
[8] G.F. Sarafanov, V.N. Perevezentsev // *Technical Physics Letters* **31(11)** (2005) 936.
[9] G.F. Sarafanov, V.N. Perevezentsev // *Physics of the Solid State* **49(10)** (2007) 1867.
[10] G.F. Sarafanov, V.N. Perevezentsev // *Technical Physics Letters* **35(4)** (2009) 302.
[11] G.F. Sarafanov, V.N. Perevezentsev, J.V. Svirina // *Technical Physics* **54(4)** (2009) 549.

[12] G.F. Sarafanov, V.N. Perevezentsev // *Physics of the Solid State* **51(12)** (2009) 2451.

[13] Yunhe Zhang, Yanfei Gao, Lucia Nicola // *Journal of the Mechanics and Physics of Solids* **68** (2014) 267.

[14] Siu Sin Quek, Zhaoxuan Wu, Yong Wei Zhang, David J. Srolovitz // *Acta Materialia* **75** (2014) 92.

[15] D.S. Balint, V.S. Deshpande, A. Needleman, E. Van der Giessen // *Materials Science and Engineering: A* **400–401** (2005) 186.

[16] D.S. Balint, V.S. Deshpande, A. Needleman, E. Van der Giessen // *International Journal of Plasticity* **24** (2008) 2149.

[17] V.S. Deshpande, A. Needleman, E. Van der Giessen // *Journal of the Mechanics and Physics of Solids* **53** (2005) 2661.

[18] H.M. Zbib, T. Diaz de la Rubia, V. Bulatov // *Journal of Engineering Materials and Technology* **124(1)** (2002) 78.

[19] B. Devincre, L. Kubin, T. Hoc // *Scripta Materialia* **54** (2006) 741.

[20] E. Van der Giessen, A. Needleman // *Modelling and Simulation in Materials Science and Engineering* **3** (1995) 689.

[21] J.G. Hirth, J. Lothe, *Theory of dislocations* (McGraw-Hill, New-York, 1968).

[22] A.E. Romanov, V.I. Vladimirov, In: *Dislocations in Solids*, ed. by F.R.N. Nabarro (North-Holland, Amsterdam, 1992), Vol 9, p. 191.

[23] V.N. Perevezentsev, G.F. Sarafanov // *Materials Science and Engineering: A* **503** (2009) 137.

[24] O. Dmitrieva, P.W. Dondl, S. Müller, D. Raabe // *Acta Materialia* **57** (2009) 3439.

[25] P. Franciosi, M. Berveiller, A. Zaoui // *Acta Metallurgica* **28** (1980) 273.

[26] O. Dmitrieva, J. V. Svirina, E. Demir, D. Raabe // *Modelling and Simulation in Materials Science and Engineering* **18** (2010) 085011.

[27] Dorothe'e Dorner, Yoshitaka Adachi, Kaneaki Tsuzaki // *Scripta Materialia* **57** (2007) 775.

[28] J.V. Svirina, V.N. Perevezentsev // *Deformation and Fracture of Materials* **N7** (2013) 2 (in Russia).